BUCKLING ANALYSIS AND QUALIFICATION STATIC LOAD TESTING OF VEGA INTERSTAGE 1/2 STRUCTURE

J. Tyrrell, J. Cremers, J. Wijker
Dutch Space B.V. (an EADS Astrium Company)
P.O. Box 32070, 2303 DB Leiden
The Netherlands

OVERVIEW

This paper presents the details of the buckling analyses and static strength testing of the Interstage 1/2 for the Vega Launch Vehicle. The Interstage 1/2 is constructed as monocoque and is buckling critical, hence the need to obtain accurate predictions for buckling strength, including the influence of initial imperfections. The buckling strength is analysed using MSC.Nastran and applying a geometric non-linear solution method. Two approaches are applied for estimation of the effects of imperfections. In the first, a knock-down factor is derived by performing a sensitivity analysis using the SRA200 program. The analysis, based on Koiter's asymptotic theory, calculates the Koiter constants "a" and "b", from which a knock-down factor is derived. In the second approach, imperfections are applied to the MSC.Nastran analysis model as the buckled form scaled to half the cone skin thickness. For this, the buckling modes are obtained from non-linear bifurcation analyses and applied as initial displacements both separately and as a "cocktail" of mode shapes in a series of geometric non-linear buckling analyses. The Interstage 1/2 was successfully qualified in April 2006 by static load test, and then in August 2006 was further loaded to final failure in a Rupture Test. The test load level at failure was found to be lower than predicted although the buckling form showed good correlation with analysis.

1. SYMBOLS AND ABBREVIATIONS

a	First post buckling coefficient
b	Second post buckling coefficient
E	Young's modulus
R	Radius
t	Wall thickness
α	Imperfection constant
β	Imperfection constant
δ	RMS Imperfection normalized with respect to the wall thickness
γ	Knock down factor
λ_c	Classical (critical) buckling load
λ_s	Reduced buckling load
$\bar{\xi}$	RMS angular imperfection amplitude (SRA definition acc. [7], page 9)
ν	Poisson's ratio
ϕ	Semi-vertex angle of cone
P_{crit}	Critical buckling load
FEM	Finite Element Model
IS1/2	Vega Interstage 1/2
SRM	Solid Rocket Motor
TNO	Netherlands Organisation for Applied Scientific Research

2. INTRODUCTION

As part of the VEGA program, Dutch Space B.V. is responsible for the design, development and manufacture of the Interstage 1/2, a cone shaped structure joining the 1st Stage P80 SRM to the 2nd Stage Z23 (Zefiro) SRM and incorporating the separation system for the 1st Stage separation.

The overall height of the Vega Interstage 1/2 is 2.1m, the Top interface ring diameter is 1.9m and the Bottom interface ring diameter 3.0m. The Interstage 1/2 is constructed from aluminium and designed and built applying conventional technologies.

The design of the Interstage 1/2 is driven by a requirement for high overall stiffness. In order to meet the stiffness requirements, a construction with relatively thick panel skins, 6.3mm is required. Doublers, thickness 3.2mm are applied around cut-outs and extend beyond the edges of the panels to form the panel interconnection joints. A monocoque aluminium construction is selected for its simplicity and because it equally meets the requirements for high stiffness, albeit that strength is then compromised through a lower buckling stability.

Many large openings exist in the Interstage 1/2 on account of the separation retro rockets and access provisions for pre-launch integration and servicing activities. These openings severely disrupt load paths through the primary load-carrying structure, so that buckling strength can not be accurately predicted using classical design formulae. Detailed geometrical non-linear analyses using Finite Element modelling techniques are therefore applied.

For a reliable prediction of the critical buckling load one must take into account expected manufacturing and assembly imperfections, also the general sensitivity of the type of structure for buckling failure.

These effects can be incorporated in the, largely empirically based, “knock-down” factors. The literature provides us with many examples of analyses and correlations with test data, from which estimates for knockdown factors can be derived. Values quoted generally range between 0.33 and 0.65, depending on the detail of analyses and tests and estimated buckling sensitivity of the structure. For the development of the Interstage 1/2 as monocoque structure with complex load paths it is considered essential that an accurate analysis of buckling stability be performed and that its sensitivity for initial imperfections be well understood.

Two approaches are applied for evaluation of the structure’s sensitivity to initial imperfections. In the first approach, a knock-down factor is derived by performing a sensitivity analysis using the SRA200 program. The analysis, based on Koiter’s asymptotic theory, calculates the Koiter constants “a” and “b”, from which the knock-down factor is derived. Two configurations of Interstage 1/2 are evaluated applying this approach, namely the monocoque construction and a version with blade stiffeners. In the second approach using MSC.Nastran no knock-down factor is used but instead the imperfections are applied directly in the analysis model as initial displacements. The displacements are modelled as the buckled form scaled to half the cone skin thickness. The scaled buckled forms of the first four modes, obtained from non-linear buckling analyses, are applied separately as initial displacements in a series of geometrical non-linear buckling analyses.

Static load tests were carried out on a qualification hardware model of the Interstage 1/2 at TNO facilities in Delft. A structural mathematical model of the complete test set-up was developed in order derive the test load correction factors and to provide final correlation of the critical buckling load and mode shape. As strength qualification, the structure was subjected to an offset compression load which induces an axial force and bending moment on the structure, such that the maximum flux is created across the weakest section of the Interstage 1/2. Two orientations of the structure were tested in this way and no failures were encountered up to qualification test load levels. Later, in a separate Rupture Test program, the structure was loaded to failure in order to establish the actual margin of safety with respect to buckling.

3. INTERSTAGE 1/2 ASSEMBLY

The Interstage 1/2 is an all-aluminium structure assembled from rolled panels and three main rings machined from forgings. Two of the rings comprise the bolted ring interfaces with the LV adjacent structures, P80 SRM and Z23 SRM, the third ring is the so-called separation ring separating “Fwd” and “Aft” Parts of the Interstage 1/2. The separation ring further accomodates the pyro-cutting cord system which is fired for 1st Stage separation, cutting through a frangible section in the ring. At 1st Stage separation the structure is cut through at the frangible section by the activation of a pyro-cutting cord device after which, six(6) Retro Rockets, positioned in the Aft Part of the Interstage 1/2, are fired to ensure that the 1st Stage is safely manoeuvred away from the 2nd Stage.

The cone-shaped Interstage structure is further stabilized against buckling by four(4) internal ringframes (three in the Aft Part and one in the Fwd Part). The ringframes are positioned to coincide with the upper and lower edges of cut-outs in order to reinforce the openings.

Cut-outs are provided in the cone panels; six(6) of these, in the Aft Part, are required for installation of the Retro Rockets, while four(4) additional openings are provided to allow access to internal equipments for integration activities. 3.2mm thick aluminium doublers are riveted to the cone panel skin as reinforcement around the cut-outs but also to provide lap joints as means to interconnect the panels. The cut-outs are further reinforced by longitudinal Z-shaped stiffeners bolted along the meridional edges of the openings. Twelve(12) stringers are thus provided in the Aft Part, reinforcing the six(6) Retro Rocket openings and four stringers are provided in the Fwd Part reinforcing two access openings.

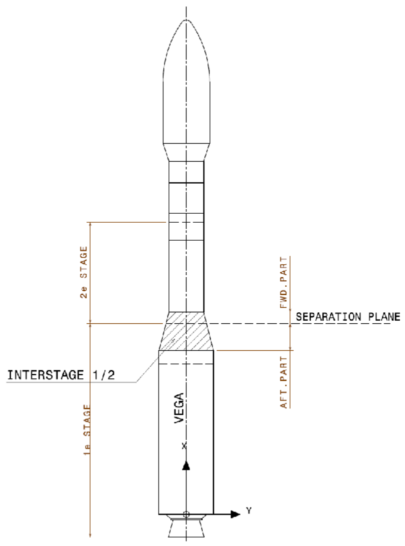

FIG 1. Vega Launch Vehicle showing position of Interstage 1/2

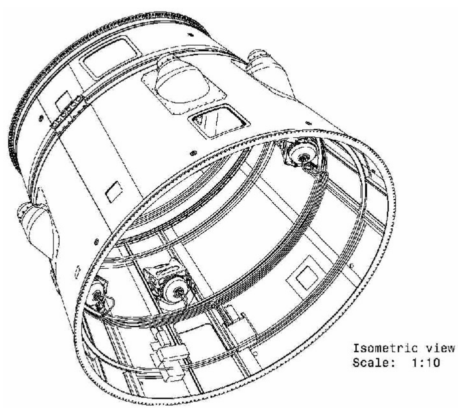

FIG 2. Geometrical model of Interstage 1/2

4. IMPERFECTION SENSITIVITY ANALYSES

4.1. Classical buckling load

The classical buckling load of a truncated unstiffened perfect conical structural member loaded with a uniform running load along the edge with the smallest radius is acc. [2] :-

(1) $$P_{crit} = \frac{2\pi E t^2 \cos^2\phi}{\sqrt{3(1-\nu^2)}}$$

A so-called “knock down factor” $\gamma \le 1$ is generally applied to the result from equation (1) to take into account the imperfection sensitivity of thin walled conical structures. Multiplied by this knock down factor, the buckling load then represents a safe but very conservative estimate.

The estimate for knock down factor obtained from [2] is $\gamma = 0.33$. This applies for truncated unstiffened perfect cones under uniform applied loads and with semi-vertex angle $10^o \le \phi \le 75^o$. From [3], however, an alternative estimate for knock down factor γ can be obtained applying the expression:-

(2) $$\gamma = \frac{0.83}{\sqrt{1+0.01\frac{\rho_1}{t}}} \qquad \frac{\rho_1}{t} \le 212$$

(3) $$\gamma = \frac{0.70}{\sqrt{0.1+0.01\frac{\rho_1}{t}}} \qquad \frac{\rho_1}{t} > 212$$

where $\rho_1 = \frac{R_{\min}}{\cos\phi}$.

The Interstage 1/2 cone semi-vertex angle, ϕ is 14.17° , smallest radius, $R_{\min} = 0.975$ m and thickness, *t* is 6.35mm, from which $\frac{\rho}{t} = 158.4$. The corresponding knock down factor applying equation (2) is $\gamma = 0.516$.

4.2. Asymptotic post buckling theory

The asymptotic post buckling theory of W.T. Koiter [4] is applied to investigate the imperfection sensitivity of the VEGA Interstage 1/2 structure. The asymptotic post buckling approach, illustrated in Fig. 3, consists of the following steps:-

1) Determine the stability of equilibrium at the lowest bifurcation point (λ_c) on the equilibrium path (see Fig.3 a),
2) Determine the sensitivity to initial geometric imperfections (λ_s) of the maximum load-carrying capacity of the structure, see Fig.3 b.

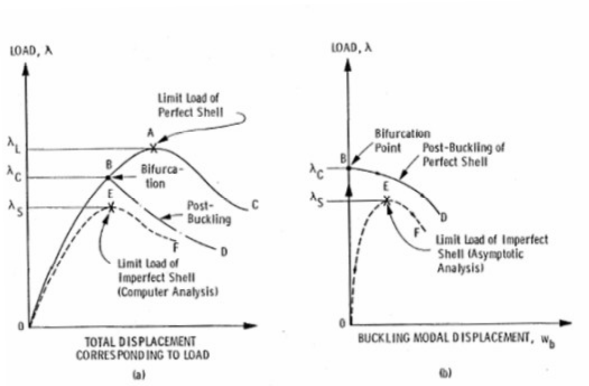

FIG 3. Load-deflection curves showing limit and bifurcation points. a) general nonlinear analysis, b) asymptotic analysis

We have to solve the following equation to obtain the ratio λ_s / λ_c [5]

(4) $$(1-\lambda_s/\lambda_c)\xi + a\xi^2 + b\xi^3 = \lambda_s/\lambda_c \delta$$

The structure is imperfection-sensitive when $a\delta < 0$ and the combination $a = 0$ and $b < 0$ [5]. We investigate the combination $a = 0$ and $b < 0$ for the case of a conical shell.

The calculation of knock down factors applying Koiter’s asymptotic theory is described in [4]. The so-called Koiter’s constants *a* and *b* are calculated using the SRA programme [6] written by Gerald A. Cohen.

In [8] the following asymptotic expansion is investigated

(5) $$(\lambda_s/\lambda_c - 1)\xi = a\xi^2 + b\xi^3 - \alpha\bar{\xi} - \beta(\lambda_s/\lambda_c - 1)\delta$$

Equation (5) is an extension of equation (4).

In [8] expressions are provided to calculate the constants *a*, *b*, α and β.

For the conditions $a = 0$ and $b < 0$ equation (4) becomes:-

(6) $$(1-\lambda_s/\lambda_c)^{\frac{3}{2}} + \frac{3}{2}\left(-3b\alpha^2\bar{\xi}^2\right)^{\frac{1}{2}}\left[\frac{\beta}{\alpha}(1-\lambda_s/\lambda_c) - 1\right] = 0$$

The imperfection parameter $\bar{\xi}$ is related to the physical RMS normalized imperfection δ as follows:-

(7) $$\bar{\xi} = \frac{\delta \cdot t}{C}$$

The factor C is calculated by the SRA program

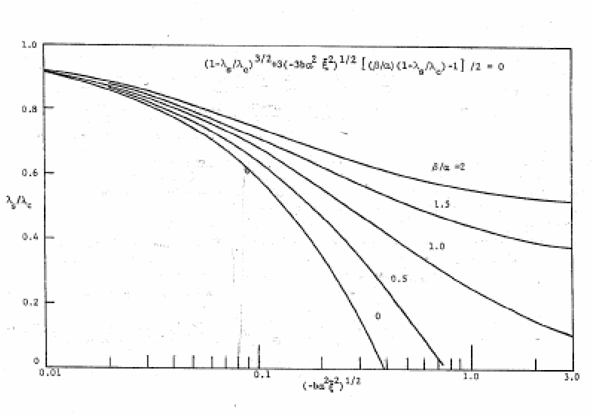

FIG 4. Critical loads of imperfection sensitive structures:

[Plots of λ_S/λ_C vs $\left(-b\alpha^2\bar{\xi}^2\right)^{\frac{1}{2}}$ for various ratios of β/α]

4.3. Analyses applying SRA programs

The imperfection sensitivity analyses are performed applying the following series of SRA programs:-

SRA 200 computes the non-linear large deflection stress and displacement response to axisymmetric torsion-less loads. The non-linear response is computed by an iterative process based on Newton's method

SRA 201 is used to determine the asymmetric (harmonic) buckling modes of axi-symmetric torsionless pre-buckling states. Geometrically speaking, the method used consists of seeking bifurcation of fictitious equilibrium states on the tangent to non-linear load-deformation curve at a load level λ.

SRA 202 is used to determine the initial post buckling behaviour and imperfection sensitivity of unique harmonic bifurcation buckling modes of axi-symmetric torsionless pre-buckling states. The program is based on Koiter's first-order imperfection theory which predicts the buckling load knock down λ_s/λ_c due to small imperfections in terms of the second post buckling coefficient *b* and imperfection values α, β and C. The knock down factor can be obtained from FIG. 4.

Two configurations of Interstage 1/2 are analysed, namely the monocoque and a stringer-stiffened version. (The stringer-stiffened version is analysed as trade for an alternative design concept for which the panels would be manufactured by shot-peening).

4.3.1. SRA analysis models

For the SRA analyses of the stringer-stiffened structure, the Interstage 1/2 is assumed to have 72 longitudinal stringers in the Aft Part and 60 stringers in the Fwd Part. The overall dimensions of the monocoque and stringer-stiffened structure are the same and are as follows:-

- Bottom radius R=1490mm
- Top radius R=927mm
- Meridional length L=2211mm

The main interface rings and intermediate ring frames are modelled by their representative areas, second moments of area and off-sets from the generator.

The cone is simply supported at its base and radially supported at the Top I/F Ring.

Elasticity modulus E=70GPa and Poisson's ratio $\nu = 0.3$

A skin thickness t=6.35mm is applied for the monocoque version but, for the stringer-stiffened version, the skin thickness is reduced to 5.4mm, compensating for the material in the added stringers, thus obtaining the same cross-sectional area. The stringers in both Fwd and Aft Parts are assumed to have a height of 27mm and width 5mm.

4.3.2. SRA analysis results

Analyses are performed for an axial line load of $N = 1.5E6$ N/m applied at the Top ring.

The results of the two sets of analyses are summarized in the TAB 1.

Paramete r	Value calculated by SRA	
	monocoque	Stringer stiffened
λ_C	1.1902	1.429
N_C	1.785*10^{6}N/m	2.144*10^{6}N/m
n	14	12
b	-11242	-2123
α	0.1519	0.2031
β	0.2149	0.1850
C	0.3520	0.2815

TAB 1. SRA analysis results for monocoque and stringer-stiffened IS1/2 cone structures

Having determined the values of the coefficients, we can solve equation (6).

The knock down factors λ_s/λ_c (knf) are presented in FIG. 4 as function of the RMS imperfection δ, normalized with respect to the wall thickness.

($\delta = 100$% means that the RMS imperfection is equal to the cone skin thickness).

The imperfection sensitivity trends are shown in FIG. 4 for both the monocoque and stringer-stiffened shells. The stringer-stiffened conical shell shows generally lower knock down factors due to imperfections. Furthermore, the classical buckling is approximately 20% higher for a stringer-stiffened cone.

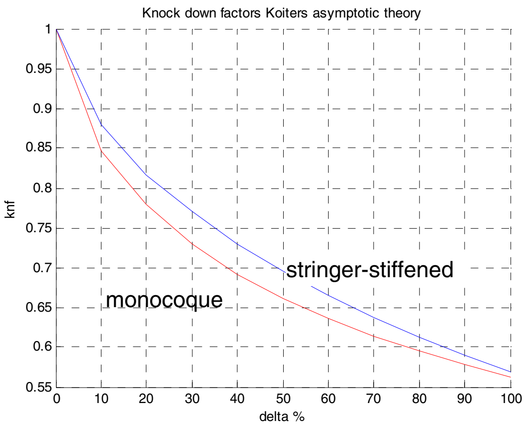

FIG 5. Comparison imperfection sensitivity monocoque and stringer stiffened shel

5. FINITE ELEMENT ANALYSES

5.1. Structural mathematical model

The structural mathematical model is a high fidelity MSC.Nastran model, representing all structural elements of the Interstage 1/2. Panels are modelled applying CQUAD4 shell elements, and the three main rings are represented by CHEXA solid elements; thus the offset at the ring connection joint is realistically modelled for buckling analysis.

The ring frames are modelled as CBEAM elements with appropriate section properties.

CBEAM elements are also used to model the stiffeners running along the edges of the openings

Equipments and retro rocket units are included in the structural mathematical model as concentrated masses (CONM2), so that local inertia loads can be combined with the main thrust loads in analyses of the structure.

The following table presents the maximum total number of Grid points and Elements in the model of the Vega IS1/2

Type of card	Total Number
GRID	63669
CQUAD4	31262
CONM2	110
CBEAM	736
CHEXA	16558

TAB 2. Quantities of elements and GRIDS used in FEM

5.2. Buckling analyses of flight configuration

Linearized and non-linear buckling analyses are performed in MSC.Nastran applying the detailed structural mathematical model. The boundary conditions represent the flight configuration, i.e. the local flexibilities of the structures adjacent to Top and Bottom rings are modelled by including portions of the Z23 SRM and P80 SRM Stages in the overall model.

The SOL 106 solution method of MSC.Nastran is applied for the nonlinear buckling analysis. MSC.Nastran provides SOL 106 as a "structured" solution sequence for nonlinear static analysis, which facilitates restarts from intermediate analysis results.

This sequence provides an incremental procedure (conventional Newton-Raphson's method) and path-following procedures (Arc-Length methods). The nonlinear equations are solved by continuation methods, also known as incremental-iterative methods or path-following methods. These methods are designed to compute the load-deformation paths from the governing (discretised) equations.

For the analyses, the worst combination of flight loads is applied. This consists of the main thrust, shear and bending moment on the structure, supplemented by local inertia loads on equipments and aerodynamic loads on protuberances. A “surflux” component corresponding to 15% of the maximum compressive flux on the Top I/F flange is also included, allowing for peak loads from the Z23 adjacent structure.

The buckling analysis is performed in two mains steps.

A nonlinear buckling analysis is first performed applying an “envelope” load case comprising a uniform compressive load simulating the maximum flux at the Top Ring I/F. The purpose of this analysis is two-fold:- Firstly, we use it to identify the weakest side or section of the structure so that the loading direction can be determined for subsequent analyses applying a “worst-case” combination of axial, shear loads and bending moment. The second purpose, or usage, is the determination of the buckling mode shapes to be applied as assumptions for the shape of initial imperfections in the cone structure.

Having established which side of the Interstage 1/2 is most sensitive for buckling failure, the worst loads combination is set up so that the maximum shear load and bending moment produce maximum compressive flux in that side of the structure. The 15% surflux supplement, equipment inertia and aerodynamic pressure loads are added to complete the load set which is then applied in a second series of buckling analyses. In this series, initial imperfections are simulated based on the buckling mode shapes computed from the first analysis with uniform axial load.

The flight limit levels of the main axial, shear loads and bending moment are applied as initial loads in the buckling analyses. These loads are applied at the centre of the Top Ring I/F flange which is not a physical point on the structure but which is connected to the flange at 360 points around its circumference by “RBE2” rigid body elements. The grid point at the centre of the ring represents the independent node and the connection points around the ring are the dependent nodes. Loads applied at the independent grid point are thus distributed along the edge of the top I/F ring. The radial translational d.o.f. of the dependent nodes is not restrained, so the Top ring is free to deform in radial direction.

The series of buckling analyses applying flight loads and initial imperfections consists of five analysis runs. In four of these runs a buckling failure mode derived from the first series of runs with “enveloped” load and scaled to a maximum deformation of a half skin thickness is applied as initial imperfection. The scaling of the buckling form to a half skin thickness, 3.15mm represents a conservative estimate justified by manufacturing and assembly tolerances of actual qualification hardware. In a fifth and final run, the four buckling modes are combined as imperfection, again scaled to a half skin thickness.

Mode #.	Buckled form
1	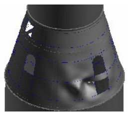
2	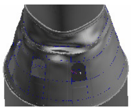
3	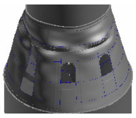
4	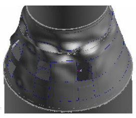

TAB 3. Mode shapes obtained from buckling analysis applying uniform axial load (mode shapes applied as initial imperfections in series of analyses with combined “worst-case” loading)

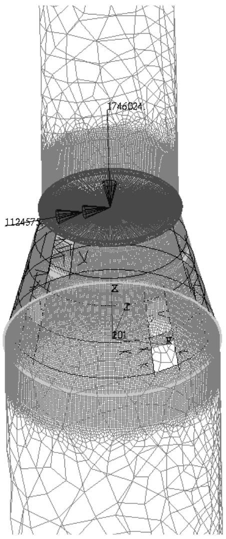

FIG 6. FE model of IS1/2 and adjacent structures showing load application of axial thrust load and bending moment.

The results of the buckling analyses applying “worst case” combined loading are given in TAB 4. In the first column the mode shapes (from the first analysis) used as basis for initial imperfection are listed, The second column presents the reserve factor of the calculated critical buckling load as a multiplier of the applied flight limit load levels.

Imperfection mode shape #	Reserve factor (1st failure mode)	Buckled form
1	1.381	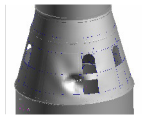
2	1.549	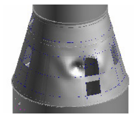
3	1.644	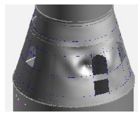
4	1.392	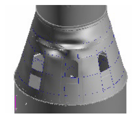
Combined (1+2+3+4)	1.550	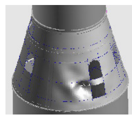

TAB 4. Results of Nastran geometrical nonlinear buckling analyses applying SOL 106

6. TEST CAMPAIGN

Static testing of the IS1/2 was split into two separate campaigns, using the same test jig and test facility at TNO-Centre for Mechanical and Maritime Structures Delft, The Netherlands. The first test conducted in April 2006 was the qualification test of a qualification model of the IS1/2. After correlating the FE model to the test data, testing was resumed in August 2006, this time with the purpose of testing the structure to final failure.

6.1. Test jig

The test jig is constructed in steel, including upper and lower adapter cylinders, simulating the adjacent structures. Construction of the test jig allows application of the main thrust load as an axial load along the launcher axis but also as load offset from the launcher axis. The offset from launcher axis is calculated to provide the required axial thrust and bending moment simulating flight qualification conditions. For characterization of overall stiffness properties, the IS1/2 was tested for pure axial load and eccentric loading for two orientations of the test article, one of which corresponded with the worst loading direction for buckling stability.

Since the analyses identified a likelihood of buckling failure occurring in regions adjacent to the Retro Rocket openings, provisions were included in the test set up to apply an additional load on one of the Retro rockets, effectively taking into account the inertia load of this item and the drag and aerodynamic pressure loads on the Retro Rocket fairing.

The test article is loaded by hydraulic jacks pulling on a central column positioned internally in the test set-up; the load is transferred into the test article through a 150mm thick circular steel plate fixed on the top boundary cylinder. An additional hydraulic jack inside the test set-up applies a load on a retro rocket assembly to simulate local equipment inertia and fairing pressure loads at one of the openings. The extra load is applied in the direction of the Retro Rocket thrust vector with a component force acting normal to the skin surface.

6.2. Test correction factors

A qualification test is the final step in the verification process of a structure under mission conditions. The qualification must cover conditions such as elevated temperatures during flight when material properties are degraded but also provide validation for minimum manufacturing tolerances and the differences between actual flight and test jig boundary conditions. Particularly for a structure which is buckling-critical, the boundary conditions can have a major impact on the critical load and failure mode. Therefore extra analyses are carried out on the structure in the test configuration to determine so-called "correction factors" for application to the test loads.

The requirements for derivation of correction factors are specified in Vega project documentation, following the methodology used for the development of the Ariane 5 launcher,

The corrected test loads are expressed by the equation:

(8) $P_Q = P_{\lim} * j_C$

where: P_Q is applied test load (qualification level)

$P_{\lim}$ is applied limit load

(9) $j_C = \left(j * K_{\min} * K_{adj} + K_T \right) * \dfrac{1}{K_\theta * K_\sigma}$

j_C is the corrected safety factor applying j =1.25 for ultimate failure due to general buckling.

The constituent factors $K_{\min}$ and K_T cover thickness tolerance and temperature gradient effects and K_θ and K_σ are material allowable corrections. The remaining factor K_{adj} represents the correction that must be made for the difference between flight and test boundary conditions and is obtained by comparing the results of analyses performed for the IS1/2 under flight and test set-up conditions. $K_{adj} \geq 1.0$, therefore this factor, like the others, also leads to an increase in the applied test load required to qualify the structure.

6.3. FE analyses of test set-up

The FE model of the test set-up includes a detailed representation of the top and bottom boundary cylinders and the base structure.

The buckling analyses to determine K_{adj} were limited to linear bifurcation analyses applying the Nastran SOL 105 solution method and disregarding initial imperfections. Although this approach can be expected to yield optimistic results, it is considered adequate to characterize the difference between test and flight boundary conditions.

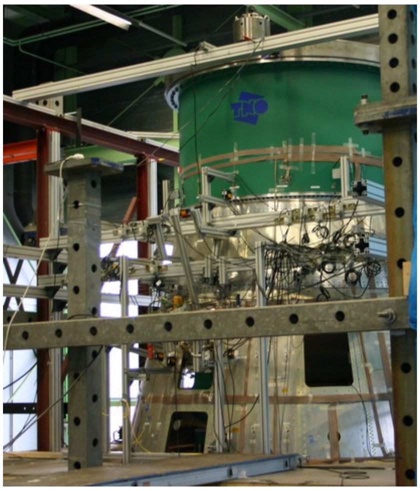

FIG 7. Interstage 1/2 qualification model in test set-up

Analysis of the test article considers the application of the main eccentric compression load combined with the load on the Retro Rocket, while the analysis of the flight configuration includes the equipment inertia loads, fairing pressure loads and surflux contributions. Results of the analyses, expressed as reserve factors of the applied limit load, are as follows:-

For flight configuration, $P_{crit} = 2.25 \cdot P_{\lim}$

For test configuration, $P_{crit} = 2.51 \cdot P_{\lim}$

The test jig factor, K_{adj} is the ratio of the buckling critical loads calculated for the test and flight configurations of the IS1/2, i.e :

$$K_{adj} = \frac{P_{crit,test}}{P_{crit,\,flight}} = \frac{2.51}{2.25} = 1.12$$

Since general buckling is an ultimate failure condition, the safety factor j =1.25 is applied. From equation (9), applying all the correction factor contributions $K_{\min}, K_{adj}, K_T, K_\theta$ and K_σ, the corrected safety factor j_C is found to be 1.53, i.e. qualification ultimate test load, $P_Q = P_{\lim} * 1.53 = 1743 \cdot 1.53 = 2667$ kN

6.4. Static Test results

The Interstage 1/2 was qualification tested applying the corrected ultimate test load P_Q of 2667KN at an offset 645mm from the launcher X-axis.

In the rupture test subsequently performed in August 2006, the Interstage 1/2 was tested to the collapse load of 3034kN. The failure mode was general buckling in the Fwd part, extending to the Aft Part in the region just below the separation ring. The structure was inspected after failure with the following observations:-

1) Intermediate ring in Fwd Part severely distorted (buckled) at three(3) locations,
2) Separation ring deformed at frangible section, convex form,
3) Fwd and Aft panels close to separation ring deformed into circumferential waveform.

The buckled panel deformations are mapped by contour lines drawn on the hardware, as shown in FIG. 8. The failure mode corresponds well with the 4th buckling mode predicted by analyses of the flight structure. This mode does not give the lowest buckling load but, as can be seen from TAB 4, the corresponding critical buckling load, reserve factor 1.392 is very close to the lowest value calculated (mode 1 with reserve factor 1.381).

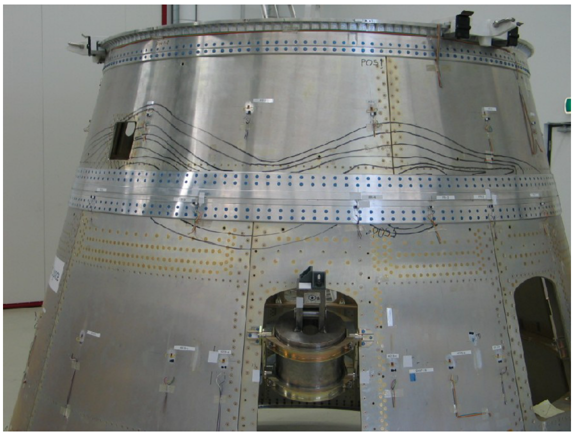

FIG 8. Deformed Interstage 1/2 structure after failure due to general buckling. (Each contour line represents 0.5mm deformation)

No failure or permanent deformation was identified in the region adjacent to the retro-rocket openings, the area where first buckling was predicted.

6.5. Correlation between test and FE analyses

Nonlinear buckling analyses applying the FE model of the test set-up and the initial imperfections modeled as a mix of the first four buckling modes scaled to a half skin thickness resulted in a buckling critical load, $P_{crit} = 2.5 \cdot P_{\lim}$, i.e. 4357kN. This is an overestimation of the collapse load, 3034kN. The FE model was therefore modified to represent the neutral surface offset of the cone panels and the analyses repeated. Results then obtained for nonlinear analyses with and without initial imperfections modelled as a mix of the first four buckling modes are as follows:-

With imperfections: $P_{crit} = 2.0 \cdot P_{\lim} = 3486$ kN

Without imperfections: $P_{crit} = 2.14 \cdot P_{\lim} = 3730$ kN

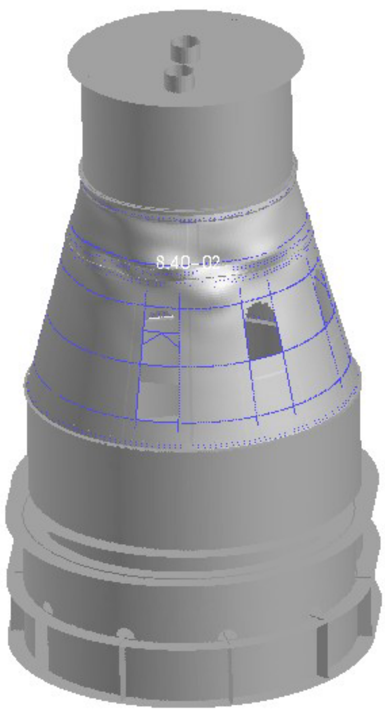

FIG 9. Analysis result for general buckling of IS 1/2 in test configuration (correlated FE model)

Comparing the above results, we see that the modelling of the panel neutral panel offsets has a significant effect, leading to a 20% lower, more accurate estimate for the buckling load, however, the analysis result is still approximately 15% higher than the test result. An explanation for this could be that the modelling of the imperfections by buckling modes is too optimistic. Comparing the test collapse load, 3034kN with the analysis result, 3730kN obtained for the analysis done without the initial imperfections, we see that the effective knock-down factor is 0.81.

7. CONCLUSIONS

The sensitivity of the IS1/2 monocoque cone has been analysed applying Koiter's asymptotic post buckling theory in calculations performed in the SRA programs. Results are compared with an equivalent stringer-stiffened structure and both configurations show moderate sensitivity to imperfections although a stringer-stiffened structure is found to be the less sensitive of the two. On the basis of the SRA analyses and assuming an RMS imperfection of 50% of the skin thickness, a knock-down factor of approximately 0.7 can be justified for the IS1/2 or similar type of structure.

In detailed MSC.Nastran FE analyses of the IS1/2 applying the geometrical non-linear solution method SOL 106, initial imperfections were introduced as buckling modes scaled to a half skin thickness. The analyses of both flight and test configurations identified the buckling mode and location in the Fwd Part where the structure finally failed during the rupture test.

The Interstage 1/2 is manufactured from relatively thick panels and this led to an overestimation of buckling strength because the neutral surface offset was not adequately represented in the FE model. During correlation of the test set-up model, the offsets were introduced into the FE model resulting in a better prediction but still an overestimation of the buckling strength.

The remaining discrepancy of approximately 15% between test and analysis suggests that the representation of initial imperfections as buckling modes scaled to half skin thickness may have been too optimistic. Comparison of the results of the analyses of the test set-up with and without initial imperfections shows an effective knock-down factor of 0.93 while the test demonstrates that the knock-down factor should not exceed 0.81.

8. REFERENCES

–

[1] C.M. Wang, ea.
Exact Solutions for Buckling of Structural Members, CRC Press, 2004

[2] Buckling of Thin-Walled Truncated Cones,
NASA SP-8019, September 1968

[3] A. Spagnoli, e.a.
Buckling Design of Stringer-Stiffened Conical Shells in Compression, , Journal of Structural Engineering, January 1999, pages 40-48

[4] W.T. Koiter,
The Stability of Elastic Equilibrium, Technical Report AFFDL-TR-70-25, 1970

[5] B. Budiansky,
Dynamic Stability of Structures, editor G. Hermann, chapter “Dynamic Buckling of Elastic Structures: Criteria and Estimates” Pergamon Press, 1967

[6] Computer Program for Analysis of Imperfection Sensitivity of Ring-Stiffened Shells of Revolution, NASA CR-1801, 1971

Acknowledgement

The authors express their thanks to Dutch Space B.V. for permission to publish this paper. Any views expressed in this paper are those of the authors and are not necessarily those of Dutch Space B.V.